Colloid Polym Sci (2015) 293:3033–3041
DOI 10.1007/s00396-015-3696-3

ORIGINAL CONTRIBUTION

Visible and fluorescence spectroscopic studies on interaction of water-soluble anionic azo dyes with Triton X-100 in reverse micelle media

Bing Li[1] · **Yongchun Dong**[1,2] · **Peng Wang**[1] · **Guixin Cui**[1,3]

Received: 13 April 2015 / Revised: 26 June 2015 / Accepted: 1 July 2015 / Published online: 30 July 2015

Abstract A series of Triton X-100 (TX-100) reverse micelles was prepared in isooctane and characterized with respect to size, polarity, and electric conductivity. Three typical azo dyes including methyl orange (MO), Acid Black 234 (AB 234) and Reactive Red 195 (RR 195) were selected and solubilized in the water phase to investigate their interaction with TX-100 reverse micelles. Effect of water content on the spectra of these dyes in the micelles was also examined. It has been revealed from the experimental results that at low water content, MO and AB 234 may be located in the polar core but outside the water pool of the micelles. Increasing water content leads to their gradual movement towards the water pools. AB 234 may bind to the micelles more closely than MO, especially at high water content. Moreover, the stronger interaction between RR 195 and TX-100 result in the complex formation. Higher water content enhances the transition from bound RR 195 to free RR 195. It can be concluded that the spectral characteristics of the three dyes in the micelles are very different owing to the space limitation and the polarity evolution of the microenvironment of the micelles.

Keywords Azo dyes · Triton X-100 · Reverse micelle · Interaction · Spectroscopy

✉ Yongchun Dong
teamdong@sina.cn

[1] Division of Textile Chemistry & Ecology, School of Textiles, Tianjin Polytechnic University, Tianjin 300387, China

[2] Key Laboratory of Advanced Textile Composites, Ministry of Education, Tianjin Polytechnic University, Tianjin 300387, China

[3] Jiangnan Branch, China Textile Academy, Shaoxing 312071, China

Introduction

The reverse micelles are nanosized spherical aggregates formed by surfactant molecules in apolar solvent and have the ability to solubilize small amount of water or aqueous solution in their interior polar core to offer a unique and versatile water pool [1-3]. And anionic, cationic, or non-ionic surfactants can be used to make different reverse micelles. An important parameter is the molar ratio of water to surfactant, $W = [H_2O]/[\text{surfactant}]$. This ratio determines most of the structural and physical properties of reverse micelles [4]. In recent years, the reverse micelles have attracted the remarkable interest because of their diverse applications in such fields as nanoparticle syntheses, enzyme processing, dyeing of textile products, dye removal from wastewater, and others. In particular, the reverse micelle dyeing has been proven to be a better alternative to traditional water-based dyeing of fiber products to save water and reduce the contaminated wastewater from dyeing bath [5]. Moreover, the reverse micelles formed with anionic surfactants, especially Aerosol-OT (AOT) were often used for textile dyeing as the dyeing medium [6-8]. But, it is found that in anionic surfactant reverse micelles, the ionic head groups of surfactant molecules has the adverse influence on the polarity of the water pool, and the uneven polar microenvironment produced may limit the application of reverse micelles in the days to come [8-11]. It is thus believed that using non-ionic surfactants can overcome the impact of the ionic head group of surfactant molecules on microenvironment in the reverse micelle. Triton X-100 (TX-100) is an important non-ionic surfactant containing polyoxyethylene (OE) group as a hydrophilic part, which may be a chain longer than the hydrophobic part of the molecule. And there are a lot of studies on the reverse micelles formed with TX-100 in different organic solvents [3, 4, 12-18]. Because of the presence of long polyoxyethylene

group, the polar interior of reverse micellar aggregates formed with TX-100 has shown much different nature from those formed with ionic surfactants.

The interaction of dye with surfactant is very important because it is closely related to many scientific fields, especially coloration of materials [17]. The interaction of TX-100 with some ionic dyes has been studied in aqueous micellar systems [19-21]. And it is well known that azo dyes account for over half of commercial dyes used in textile industry. They can be characterized by the presence of one or more azo groups. And these dyes can provide fibers with bright and high intensity colors and have fair to good fastness properties because azo group is a powerful chromogen [22]. Some azo dyes have been used for the coloration of cotton, wool, and silk fibers in AOT reverse micelle systems, and their dyeing processes have also been investigated [6-8]. More importantly, a typical azo dye, Reactive Red 195 was used for the salt-free coloration of cotton fabric in TX-100 reverse micelle in our previous study [23]. Reactive Red 195 showed a stronger adsorption performance on cotton fabric in Triton X-100 reverse micelle than in bulk water in the absence of NaCl. Moreover, a higher fixation of the dyes absorbed on the cotton fiber was achieved when sodium carbonate was used as the alkali agent. However, there has been little information on the interaction of azo dye with TX-100 in reverse micellar system, although methyl orange has been served as an adsorption probe to examine the microenvironment of reverse micelles [17, 24, 25]. In the present work, a series of non-ionic reverse micelles was prepared with a non-ionic surfactant TX-100, *n*-octanol, and isooctane and characterized with respect to size, polarity, and conductivity. Three typical azo dyes with different structure were chosen and solubilized in TX-100 reverse micelles, respectively, for the evaluation of their interaction with the micelles in isooctane. Moreover, effect of water content on the spectra of these dyes in TX-100 reverse micelle was investigated. And position and orientation of these dyes in TX-100 reverse micelle was also discussed and compared.

Experimental

Materials and reagents

A non-ionic surfactant, Triton X-100 ($C_8H_{17}C_6H_4(OC_2H_4)_{10}OH$) was of reagent grade and used without further purification. Isooctane, *n*-octanol, and all other chemicals were of analytical grade and used as received. The three azo dyes used in this experiment were methyl orange (MO), Reactive Red 195 (RR 195) and Acid Black 234 (AB 234). MO was indicator grade product of Tianjin Nankai Chemical Reagents Co., China. Both commercial samples of RR 195 and AB 234 were supplied by Tianjin Sanhuan Chemicals Co., China. They were crystallized twice from an ethanol-water mixture before use. And the molecular structures of the three dyes are presented in Scheme 1. Double distilled and deionized water was used throughout the study.

Preparation of TX-100 reverse micelles

According to our previous work [23], TX-100 reverse micelles were prepared by a simple injection method at room temperature. TX-100 and *n*-octanol were firstly dissolved at a fixed weight ratio of 1.25:1 in isooctane to obtain a 20 mL of organic surfactant solution with a TX-100 concentration of 0.20 mol L^{-1}. Stock dye solutions were prepared by dissolving the appropriate weight of the solid dye in the boiling deionized water. And then a desired amount of deionized water or stock dye solutions were dropped into the organic surfactant solutions using a microsyringe. After the injection of stock dye solutions, the mixtures were vigorously stirred for 10 min and treated using an ultrasonic mixer until the transparent TX-100 reverse micelles were obtained. The concentration of each dye in reverse micelles was kept at 0.018 mmol L^{-1}. In order to make the reverse micellar systems with different water/surfactant molar ratio (W) values, the appropriate amounts of deionized water were subsequently added to all the systems. Maximal W value without phase separation of TX-100 reverse micellar system attained in this study was ca. 25. The molar ratio of TX-100 to dye was greater than 5.0×10^3, Thus, the perturbation of the system by the presence of the dyes may be assumed negligible [17, 25]. It should also be believed that there may be only one dye molecule in each polar core of TX-100 reverse micelle because the number of TX-100 reverse micelles is much more than that of dye molecules in the systems at different W values.

Characterization of TX-100 reverse micelles

The size (diameter and aggregation number) of TX-100 reverse micelles was estimated based on their viscosity measurement reported by Kinugasa et al. [26]. The kinetic viscosity of TX-100 reversed micelle was measured using an Ostwald viscometer in a water bath. ^{1}H NMR spectra of TX-100 reverse micelles were conducted on an Inava 500MHZ NMR spectrometer (Varian Corporation, USA) at the Analysis and Measurement Center at Tianjin University, Tianjin. And the electric conductivities for TX-100 reversed micelles determined using a DDSJ-308A conductivity meter (Shanghai Jingmi Instrumental Co., China). All the measurements were performed at 25 ± 1 °C.

UV-vis and fluorescence spectral measurements

Steady-state UV-vis absorption and fluorescence spectra of TX-100 reverse micelles were recorded using a UV-2401 Shimadzu spectrophotometer (Shimadzu Co., Japan) and a

Scheme 1 **a** Chemical structure of Triton X-100 (TX-100). **b** Chemical structure of methyl orange (MO). **c** Chemical structure of Acid Black 234 (AB 234). **d** Chemical structure of Reactive Red 195 (RR 195)

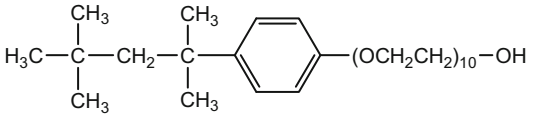

(a) Chemical structure of Triton X-100 (TX-100)

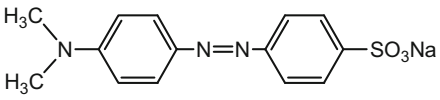

(b) Chemical structure of Methyl Orange (MO)

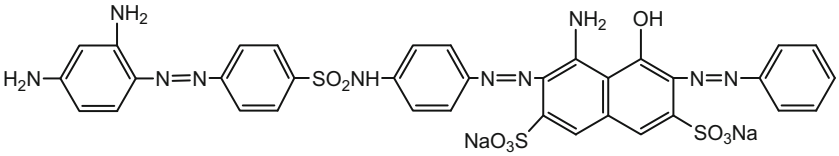

(c) Chemical structure of Acid Black 234 (AB 234)

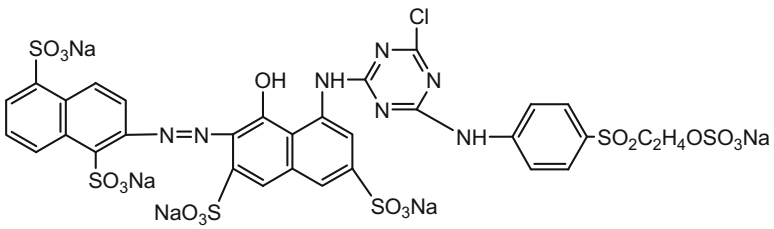

(d) Chemical structure of Reactive Red 195 (RR 195)

F-4500 fluorescence spectrometer (Hitachi Co., Japan), respectively. All spectral measurements were duplicated at 25 °C accurate to within ±0.5 °C, and the mean values were processed for data analysis.

Results and discussion

The critical micellar concentration (cmc)

The cmc is the concentration of surfactant at which micelles first appear in solution. The solubilization of water is often used in the determination of the cmc value of surfactants in non-aqueous solvent [27, 28]. In this work, different amounts of the distilled water were mixed with the TX-100/*n*-octanol/isooctane by ultrasonic mixer for a desired time to measure the cmc value of TX-100 in isooctane, and results are shown in Fig. 1.

Figure 1 shows that at a low TX-100 concentration, the solubilizing water amount varies little with TX-100 concentration. It is noted that the solubilizing water amount drastically increased at TX-100 concentrations above ca 0.003 mol L^{-1}, which is similar to the result reported in our previous work [23]. The organic phase was found to be clear and transparent, indicating that the formation of TX-100 reverse micelles was achieved. A TX-100 concentration of 0.003 mol L^{-1} was taken as cmc value of TX-100/*n*-octanol/isooctane system, which is comparable to that of TX-100 in chloroform [3].

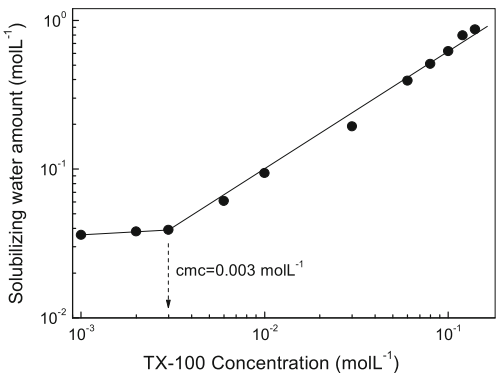

Fig. 1 Solubilizing water concentration in TX-100/*n*-octanol/isooctane organic phase at 25 °C

Characterization of TX-100 reverse micelles

Diameter and aggregation number

Micelle diameter (d_{rm}), water pool diameter (d_{wp}), and aggregation number (n_{ag}) are the three important size parameters, which determine the microenvironment and structure of reverse micelles. In this work, d_{wp} and n_{ag} of TX-100 reverse micelles were thus determined from the viscosity measurement and then d_{rm} was calculated by $d_{rm} = d_{wp} + 2L_S$, where L_S is the length of surfactant (4.45 nm for TX-100, obtained using Chemoffice software). Additionally, the mean packing density of TX-100 molecules in the micelles (p_m) was also calculated by $p_m = n_{ag}/(\pi\, d_{wp}^2)$. The variation of d_{rm}, d_{wp}, n_{ag}, and p_m values with water content was shown in Figs. 2 and 3.

Figure 2 shows that d_{rm} and d_{wp} values of TX-100 reverse micelle linearly increase with W increasing from 3 to 15. The insignificant change in both values is observed when W is above 15. Also, it should be noticed that d_{rm} value of TX-100 reverse micelles in isooctane is located in 12–19 nm range. Similar d_{rm} values were obtained for TX-100 reverse micelles in chloroform [3] and cyclohexan [15]. On the other hand, it is found in Fig. 3 that n_{ag} value increases with increasing W, and its maximum value is achieved at W = 15. Above the maximum value, n_{ag} value gradually decreases. This result is in agreement with that obtained with the TX-100/cyclohexan/water system [15] studied earlier. The main reason is that added water enhances surfactant association by bridging adjacent polyoxyethylene chains and during this process the aggregation number increases. But, with further addition of water, there is a diminishing number of solvent molecules to be displaced from the core, thus as a compensation, the aggregation number is reduced [15, 24]. Moreover, a sharp decrease in p_m value was found at $W \leq 4$. And then p_m value declined insignificantly with further addition of water. This means that TX-100 molecules are especially crowded in the reverse micelles at low water content.

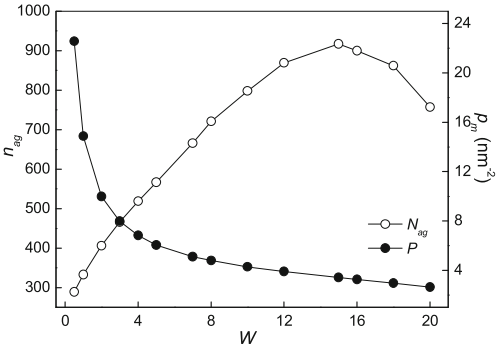

Fig. 3 Effect of water content on aggregation of TX-100 molecules in reverse micelles

NMR spectroscopic studies

Figure 4 shows that at W = 1, a small single peak is observed at about 4.33 ppm, which is due to the OH proton signal, reflecting a fast exchange between the protons of bound water and the OH protons of *n*-octanol and Triton X-100 molecules [13-14, 29]. More importantly, it is found that the chemical shift of the OH moves from 4.33 to 4.65 ppm and its peak intensity become stronger at W = 10. This is attributed mainly to the increasing polarity of the water molecules in TX-100 reverse micelle. Similar trend has been reported by Kumar and co-worker [14] for TX-100 reverse micelle in cyclohexane. This is because higher water content leads to the formation of free water in the system and significantly increases the number of hydrogen bonding between the ethylene oxide residue and water molecule, which decreases the electron density around the proton and thus moves the proton absorption to a lower field [3, 13, 14]. On the other hand, both peaks at 3.41 and 3.46 ppm are ascribed to the chemical shift of CH_2CH_2O proton for TX-100 molecules [14]. And a small change in the chemical shift indicates the

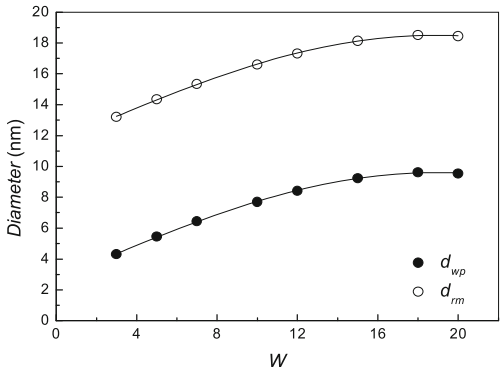

Fig. 2 Relationship between water content and size of TX-100 reverse micelle

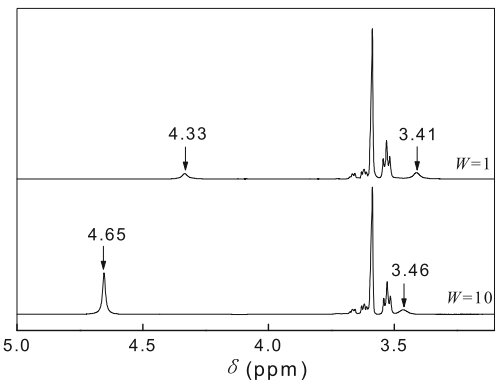

Fig. 4 ^{1}H NMR spectra of TX-100 reverse micelles at different water content

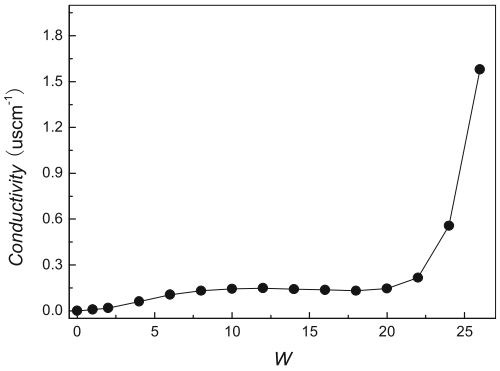

Fig. 5 Variation of conductivity with W in TX-100 reverse micelles

changed solvent environment when W increases from 1 to 10.

Electric conductivity

Figure 5 shows that the conductivity of TX-100 reverse micelle increases with W increasing until a maximum value. With further increasing W, it insignificantly decreases and then sharply increases. There are both different conducting mechanisms depending on W values. At $W < 20$, the conductivity is generally considered as the result of the charged droplets motion in the electrical field [30, 31]. At $W > 20$, higher water content significantly enhances the aggregation of the individual water droplets in solvent into the infinite clusters. And then the charge carriers move through the clusters in the electrical field and percolation conducting takes place, thus causing the high conductivity [32, 33]. Furthermore, the conductivity of reverse micelles is very sensitive to their structure. And it is generally accepted that higher water content or conductivity may increase the micelle size, attractive interactions, and the exchange of materials between water droplets [1, 34].

Absorption spectra of the three azo dyes in TX-100 reverse micelle

The appropriate amounts of deionized water were added into the TX-100 reverse micelles containing azo dye solutions with 0.036 mmol L^{-1} initial concentration to obtain a series of the reverse micellar systems with different W values. And then the absorption spectra of each dye in these systems were measured and examined.

Methyl orange

Figure 6 represents the absorption spectra of MO in TX-100 reverse micelle at different water content. And MO exhibits the varied maximum absorption wavelengths (λ_m) from 411 to 418 nm with the addition of water. Moreover, it is clearly found from Fig. 7 that A_m (the absorbance at λ_m) increases markedly with W until it reaches a stable value (0.6) at $W = 4$. Similar observations have been reported by Qi and co-workers [17] for the reverse micelle system consisting of TX-100, cyclohexane, and water and Zhu and co-workers [25] for the TX-100 reverse micelle in mixed solvents of benzene and *n*-hexane. This results suggests that at low water content ($W < 4$), MO molecules are located in the polar core but outside the water pool. MO molecule penetrates the interfacial layer of the micelle with its azo group embedded between the hydrated EO chains of TX-100 and with its terminal SO_3Na group anchored in the initial water pool. With water content increasing (at $W > 4$), the formation of the water pools with large size and high polarity begins in the micelles, which results in leaving the microenvironment of the azo group and increasing hydration of the SO_3Na group, thus enhancing its insertion and anchoring in the pool [17, 25]. Moreover, it is found from Fig. 6 that the solubilization of MO in TX-100 reverse micelles produces a red shift of ca. 7 nm, which may be due to the hydration of the azo group. This shift exhibits the variation from hydrazone to the azo tautomeric form on progressing in the gradually increasing polar media in the micelle, which is attributed to the enhanced hydrogen bonding of the azo moiety. In addition, previous researches [22, 35] have reported that when the whole dye molecule may be coplanar, the p-electron is delocalized over the conjugated system. While the dye molecule is compressed by outside force, the planarity of the dye molecule is broken and the p-electron is delocalized with difficulty. As seen from the structure formula in Scheme 1, MO molecule has two plane parts linked by

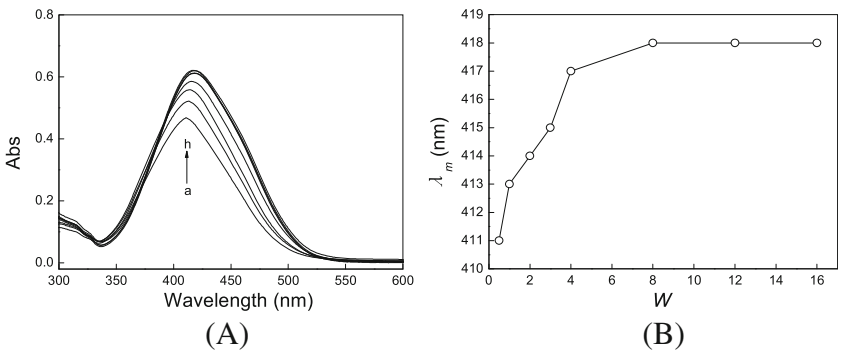

Fig. 6 **a** Effect of water content on visible absorption spectra of MO in TX-100 reverse micelles, [MO] = 0.018 mmol L^{-1}, [TX-100] = 0.20 mol L^{-1}; W: (a) 0.5, (b) 1.0, (c) 2.0, (d) 3.0, (e) 4.0, (f) 8.0, (g) 12, (h) 16. **b** λ_m of MO in TX-100 reverse micelles as a function of water content

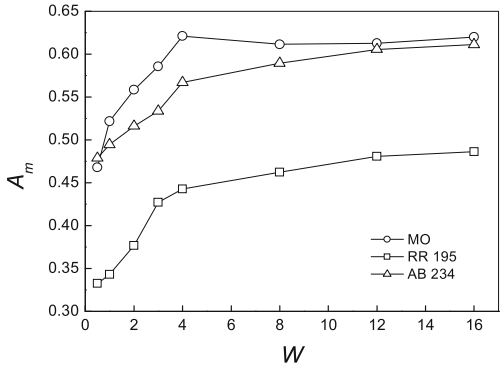

Fig 7 Variation of A_m of the three azo dyes in TX-100 reverse micelles with water content

an azo group. Additionally, the mean packing density of TX-100 molecules in the micelle (p_m) decreases with increasing water content as mentioned above (Fig. 3). Therefore, MO molecule located between the EO chains of TX-100 is significantly compressed and twisted at low water content. Thus, the conjugated system of the dye molecule is broken, reflecting in a short λ_m value. As water content increases, lower packing density may make dye molecule easily extend in the hydration shell of the micelle, thus, causing a red shift of λ_m value.

Acid Black 234

Figure 8 shows that λ_m value of AB 234 in the micelle almost linearly increases with W increasing from 0.5 to 16, which is different from that for MO at $W > 4$. And AB 234 exhibits a similar red shift to MO. It should also be pointed out that unlike MO, AB 234 exhibits a gradually increasing trend in A_m even though at $W > 4$, which is attributed to the presence of two SO_3Na groups in its molecule. A main reason for this phenomenon may be that hydration of the SO_3Na group leads to enhanced absorbance [25]. Apparently, the hydration of the SO_3Na groups reaches saturation at $W = 12$ because little change in A_m was observed after this point. These results imply that AB 234 molecule may exist between the EO chains of TX-100 in the same way as MO does. However, AB 234 possesses a bigger molecule size and higher weight than MO, especially three azo groups and two SO_3Na groups those are sensitive to changes in their local microenvironments. As a result, AB 234 may bind to the micelles more strongly than MO, particularly at high water content. Thus, it is believed that AB 234 shows the same location fashion as MO in TX-100 reverse micelles. However, the interaction of AB 234 with TX-100 is stronger than that of MO with TX100 at the same conditions because of the big difference in molecular characteristics between them.

Reactive Red 195

Figure 9 shows the effect of successive addition of water on the absorption spectra of RR 195 in the TX-100 reverse micelle. The variation in spectra of RR 195 in TX-100 reverses micelle with water content passes through one isosbestic point (574 nm), which was not found in the spectra of both dyes mentioned above under the same conditions. The presence of the isosbestic point supports the formation of a 1:l complex between RR 195 and TX-100. And there is a dye-micelle equilibrium between free RR 195 and bound RR 195 in the micelles. Moreover, as W is increased up to 4, there is an insignificant change in λ_m value, while the remarkable enhanced A_m value was observed in Fig. 7. This indicates that at low water content, water binds directly to the EO chains of TX-100 and the hydration of the complex does not break the complex between RR 195 and TX-100. As a consequence, RR 195 is present predominantly as bound RR 195. It is worth noticing that when W is increased from 4 to 8, λ_m value of RR 195 sharply increases and A_m value exhibits an insignificant increasing trend, thus leading to the dramatic transition from bound RR 195 to free RR 195 due to the formation of water pool and presence of the secondary bound water with higher polarity next to the primary hydration shell of the EO chains [17]. Further addition of water ($W > 8$) does not change λ_m value of RR 195 considerably, implying that RR 195 is saturated with water and present as its free form, which may be a

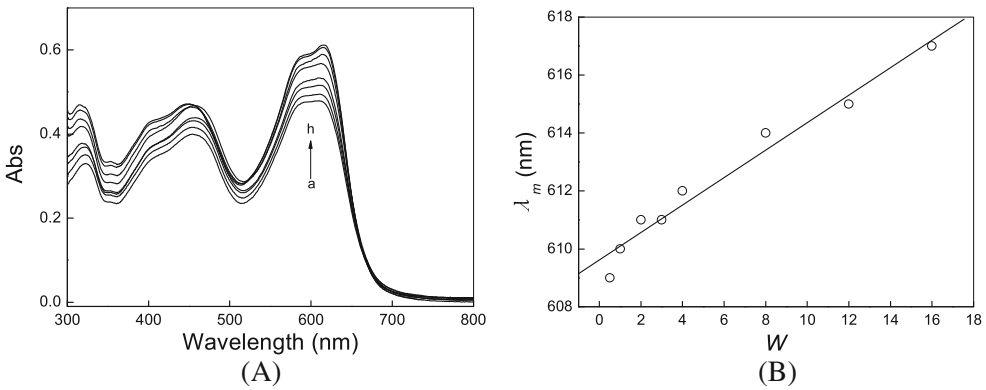

Fig. 8 **a** Effect of water content on visible absorption spectra of AB 234 in TX-100 reverse micelles, [AB 234] = 0.018 mmol L^{-1}, [TX-100] = 0.20 mol L^{-1}; W: (a) 0.5, (b) 1.0, (c) 2.0, (d) 3.0, (e) 4.0, (f) 8.0, (g) 12, (h) 16. **b** λ_m of AB 234 in TX-100 reverse micelles as a function of water content

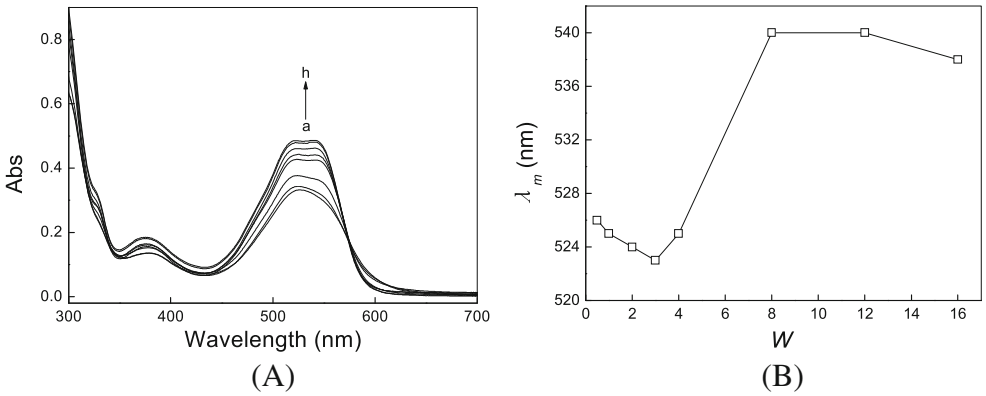

Fig. 9 **a** Effect of water content on visible absorption spectra of RR 195 in TX-100 reverse micelles, [RR 195] = 0.018 mmol L^{-1}, [TX-100] = 0.20 mol L^{-1}; *W*: (a) 0.5, (b) 1.0, (c) 2.0, (d) 3.0, (e) 4.0, (f) 8.0, (g) 12, (h) 16. **b** λ_m of RR 195 in TX-100 reverse micelles as a function of water content

reason for its better adsorption on cotton fiber [23]. And the additional water results in a larger water pool but leaves the microenvironment of RR 195, and thus λ_m value of RR 195 remains relatively constant. It has been reported that a possibility for a 1:1 complex formation between RR 195 and TX-100 inside the reverse micelles is the charge transfer interaction between the dye and the TX-100 molecules. The other possibility may be due to hydrophobic interaction between TX-100 and dye molecules [36].

Fluorescence spectra of the three azo dyes in TX-100 reverse micelles

Figure 10 shows the fluorescence emission spectra of the three dyes in TX-100 reverse micelles at different values of *W*. Different shifts of the fluorescence maximum (λ_{fm}) were found for the three dyes, which is attributed to their different locations in the reverse micelles. In the case of MO, a fluorescence emission spectrum is observed to undergo progressive blue shifts with the gradual increase in water content. An intensive λ_{fm} value appears at 351.6 nm at lowest water content ($W = 0.2$), that reaches a value of 347.0 nm at highest water content ($W = 20$), corresponding a blue shift of 4.6 nm. The emission spectrum of AB 234 is the most interesting because of the unchanged λ_{fm} value (693.4 nm) with increasing water content. These results indicate that both dyes, especially MO, are located in a region far from the water pool of the reverse micelles. The spectral changes may be due to the formation of hydrogen bond between the SO_3Na group and the water molecule in reverse micelles. Consequently, they are believed to be oriented at the interface of reverse micelles with the SO_3Na group towards the water pool, while the azo group remains

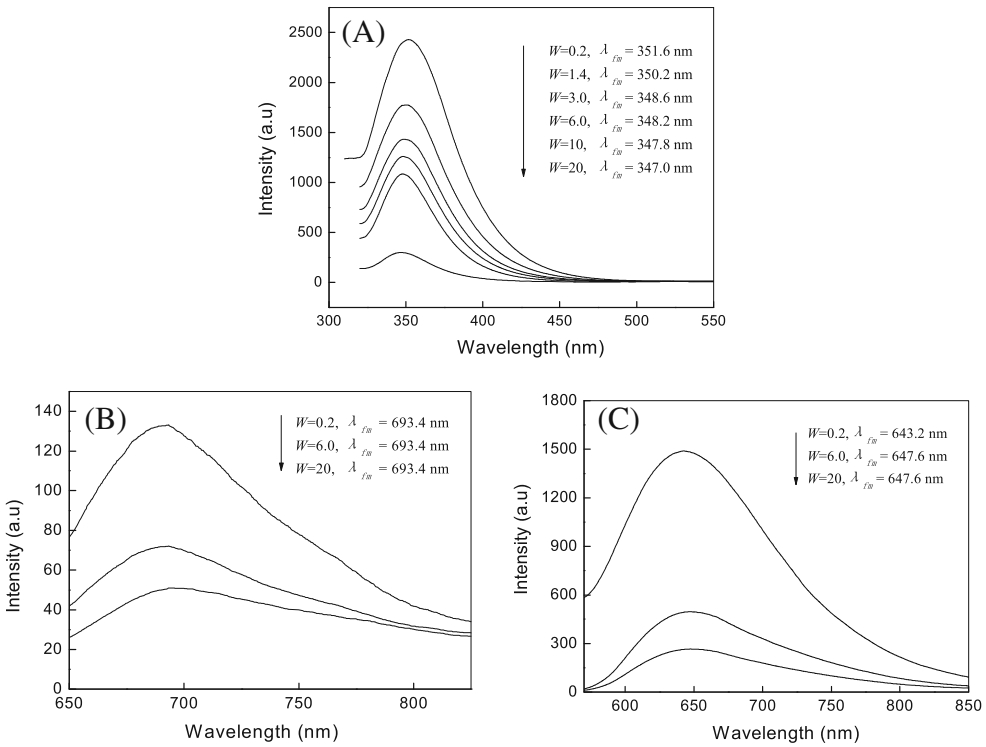

Fig. 10 Fluorescence emission spectra of the three dyes including **a** MO, **b** AB 234, and **c** RR 195 at different *W* values in TX-100/*n*-octanol/isooctane reverse micelles. [Dye] = 0.0036 mmol L^{-1}, [TX-100] = 0.20 molL^{-1}

buried at the interface as the hydration increases. The similar result is obtained for an ionic styryl dye in AOT reverse micelles [37]. In contrast, a red shift of 4.4 nm is found for RR 195 under the same conditions, suggesting that at low water content, RR 195 molecules is initially close to the head group region of the reverse micelles and increasing water content makes the dye molecules gradually enter more and more hydrated environments [38, 39]. This is consistent with the results obtained in the absorption spectrum mentioned above. Comparing the fluorescence emission spectra of the three dyes, it is found that λ_{fm} value of MO is much lower than those of the two dyes, especially AB 234. While their fluorescence intensities at λ_{fm} show a reverse trend at the same water content. These results may be owing to the big difference in molecular size and conjugated system between them. MO molecule has a smaller size and a shorter conjugated system than the two dyes. The p-electron is delocalized throughout a shorter carbon skeleton; thus, MO molecule presents a lower λ_{fm} value. However, AB 234 and RR 195 molecules may be compressed more strongly by the TX-100 molecular membrane in the reverse micelle than MO molecule because of their bigger sizes. This leads to the breaking of their molecular planarity, resulting in the low fluorescence intensity.

Conclusions

TX-100 reverse micelles were prepared by injecting the distilled water or azo dye solutions into the mixture of TX-100, *n*-octanol, and isooctane at room temperature. The cmc value of TX-100 in isooctane was determined to be 0.003 mol L^{-1}. Three important size parameters of TX-100 reverse micelles were also measured using viscosity method. Their micelle diameter and water pool diameter are lower than 20 nm and increase with water content increasing. While their aggregation number shows the similar trend and the maximum value at $W = 15$. And then the mean packing density of TX-100 molecules in the reverse micelle was calculated by the values of water pool diameter and aggregation number. NMR and electric conductivity measurement indicated the variation of microenvironment in water pool of TX-100 reverse micelle with water content. Visible and fluorescence spectra studies demonstrate that the three dyes were located in the TX-100 reverse micelle in the different modes, which is dependent highly upon their molecular structures. Higher water content caused a significant red shift in λ_m values of MO and AB 234 in the micelles. And a remarkable increase in A_m values of the three dyes in the micelles was found at low water content ($W \leq 4$). Increasing water content led to a dramatic reduction in fluorescence intensity of the three dyes in the micelles. However, they exhibited the totally different changes in λ_{fm} values as water content increases. These findings suggests that at low water content, MO and AB 234 may be located in the polar core but outside the water pool of the micelles. Increasing water content can enhance their gradual movement towards and insertion in the pools. However, the interaction of AB 234 with TX-100 is stronger than that of MO with TX-100, particularly at high water content due to the big difference in molecular characteristics, especially the number of azo groups and SO_3Na groups between them. An isosbestic point in the spectra of RR 195 indicated the formation of a 1:l complex between RR 195 and TX-100. Higher water content greatly enhanced the transition from bound RR 195 to free RR 195. In addition, AB 234 and RR 195 with bigger molecular sizes show the lower fluorescence intensity than MO in the micelles at the same water content, which may be attributed to their significant twisting or breaking of their molecular planarity caused by the stronger compression from the TX-100 molecular membrane in the micelles.

Acknowledgments The authors thank the Tianjin Municipal Science and Technology Committee for a Science and Technology Support Key Project Plan (09ZCKFSH02000). This research was also supported by Zhejiang Province Science and Technology Program Foundation (2007C16033).

References

[1] Liu D, Ma J, Cheng H, Zhao Z (1998) Colloids Surf A 135:157
[2] De TK, Maitra A (1995) Adv Colloid Interf Sci 59:95
[3] Dhar S, Rana DK, Sarkar A, Mandal TK, Ghosh S, Bhattacharya SC (2009) Colloids Surf A 349:117
[4] Jaramillo N, Paucar C, García C (2014) J Mater Sci 49:3400
[5] Sawada K, Ueda M (2003) Dyes Pigments 58:37
[6] Sawada K, Ueda M (2003) Dyes Pigments 58:99
[7] Sawada K, Ueda M (2003) Color Technol 119:182
[8] Sawada K, Ueda M, Kajiwara K (2004) Dyes Pigments 63:251
[9] Ueda M, Kimura A, Wakida T, Yoshimura Y, Schelly ZA (1994) J Colloid Interface Sci 163:515
[10] Sawada K, Ueda M (2004) J Chem Technol Biotechnol 79:376
[11] Sawada K, Ueda M (2004) J Chem Technol Biotechnol 79:369
[12] Kumar C, Balasubramanian D (1979) J Colloid Interface Sci 69: 271
[13] Kumar C, Balasubramanian D (1980) J Colloid Interface Sci 74:64
[14] Kumar C, Balasubramanian D (1980) J Phys Chem 84:1895
[15] Zhu DM, Feng KI, Schelly ZA (1992) J Phys Chem 96:2382
[16] Das SK, Ganguly BN (1997) J Colloid Interface Sci 192:184
[17] Qi L, Ma J (1998) J Colloid Interface Sci 197:36
[18] Das D, Nath DN (2007) J Phys Chem B 111:11009
[19] Dutta RK, Bhat SN (1996) Colloids Surf A 106:127
[20] Mukhopadhyay M, Varma CS, Bhowmik BB (1990) Colloid Polym Sci 268:447
[21] Bhowmik BB, Mukhopadhyay M (1998) Colloid Polym Sci 266: 672
[22] Perkins WS (2004) Beijing: China Textile Press.
[23] Yi SX, Dong YC, Li B, Ding ZZ, Huang XB, Xue LX (2012) Color Technol 128:306–314
[24] Zhu DM, Schelly ZA (1992) Langmuir 8:48
[25] Zhu DM, Wu X, Schelly ZA (1992) J Phys Chem 96:7121
[26] Kinugasa T, Kondo A, Nishimura S, Miyauchi Y, Nishii Y, Watanabe K, Takeuchi H (2002) Colloids and Surf A 204:193

[27] Naoe K, Nishino M, Ohsa T, Kawagoe M, Imai M (1999) J Chem Technol Biotechnol 74:221
[28] Naoe K, Ura O, Hattori M, Imai M (1998) Biochem Eng J 2:113
[29] Yoshida T, Okabayashi H, Takahashi K, Ueda I (1984) Biochim Biophys Acta 772:102
[30] Eicke HF, Borkovec M, Das-Gupta B (1989) J Phys Chem 93:314
[31] Giustini M, Palazzo G, Colafemmina G, Monica MD, Giomini M, Ceglie A (1996) J Phys Chem 100:3190
[32] Feldman Y, Kozlovich N, Nir I, Garti N, Archipov V. Idiyatullin Z. Zuev Y. Fedotov V (1996) J Phys Chem 100: 3745.
[33] Maitra A, Mathew C, Varshney M (1990) J Phys Chem 94: 5290
[34] Hou MJ, Kim M, Shah DO (1988) J Colloid Interface Sci 123:398
[35] Zhang Z, Liu C (2000) J Photochem Photobiol A 130(2):139
[36] Pramanick D, Mukherjee D (1993) J Colloid Interface Sci 157:131
[37] Sahoo D, Chakravorti S (2009) J Photochem Photobiol A 205:129
[38] Sengupta B, Guharay J, Sengupta PK (2000) Spectrochim Acta Part A 56:1433
[39] Zang L, Liu CY, Ren XM (1995) J Photochem Photobiol A 88:47